# Pressure and Temperature Dependence of Glass-Transition Dynamics in a "Fragile" Glass Former

G. Li,[1] H. E. King, Jr.,[2] W. F. Oliver,[3] C. A. Herbst,[2,*] and H. Z. Cummins[1]

[1]*Department of Physics, City College, City University of New York, New York, New York 10031*

[2]*Corporate Research Science Laboratories, Exxon Research and Engineering Company, Route 22 East, Clinton Township, Annandale, New Jersey 08801*

[3]*Department of Physics, University of Arkansas, Fayetteville, Arkansas 72701*

(Received 15 August 1994)

A depolarized light-scattering study of isopropylbenzene has been carried out at pressures from 1 bar to 7.6 kbar and at temperatures from 293 to 122 K. Both the supercooled and superpressed liquids show two-step relaxation processes. The faster relaxation in both cases can be described by a mode-coupling $\beta$ relaxation theory. Comparison of the pressure and temperature data indicate that density is not the only relevant parameter required to explain the evolution of the $\beta$ relaxation dynamics as the liquid-glass transition is approached.

PACS numbers: 64.70.Pf, 07.35.+k, 66.20.+d, 78.35.+c

For many glass-forming materials, a liquid-glass transition can be induced either by decreasing the temperature through a glass-transition temperature $T_g$ or by increasing the pressure through a glass-transition pressure $P_g$. In the latter class of experiments, relaxation rates were first obtained by Bridgman [1] who measured the viscosity of several liquids up to 30 kbar. Later, viscosity measurements were extended to higher pressures through the use of multianvil presses and diamond anvil cells (DAC's) [2]. Dynamical information has also been obtained in liquid-glass-forming systems up to 90 kbar in the frequency range 0.1 to 450 kHz via dielectric relaxation [3], and at frequencies as high as 150 MHz in the pressure regime $P < 5$ kbar by ultrasonic absorption [4]. Light-scattering techniques in the DAC have been used much more recently to measure high-pressure relaxation times in the GHz regime up to 120 kbar [5]. However, the great majority of studies of liquid-glass dynamics have been performed with isobaric temperature scans due to the relative difficulty of high-pressure measurements. In particular, no pressure-scan experiment has heretofore been reported in the frequency range required to test the mode-coupling theory (MCT), which predicts a fast $\beta$ relaxation regime [6] located between the low-frequency $\alpha$ relaxation and the high-frequency microscopic excitation band.

For the temperature-induced liquid-glass transition, several neutron scattering [7] and depolarized light scattering [8] measurements of some fragile glass-forming materials observed the two-step relaxation process in the supercooled liquid near the liquid-glass transition. The fast relaxation processes are found to follow the scaling law predictions of the MCT $\beta$ relaxation process. It is of critical interest to determine whether the evolution of $\beta$ relaxation dynamics with varying temperature and varying pressure follow a similar pattern, and whether the MCT can be applied for both cases. For temperature- and pressure-induced glass-transition processes, the density changes via thermal expansion and compressibility, respectively. Therefore, an important question is whether density is the dominant parameter for the liquid-glass transition dynamics or if thermal effects also play an important role. A deeper understanding of the liquid-glass transition requires information on the role played by both parameters.

To address these questions, we have carried out a wide-frequency-range depolarized-light-scattering study of isopropylbenzene (cumene) [$C_6H_5CH(CH_3)_2$, $T_m = 177$ K, $T_g \simeq 125$ K] with varying pressure at $T = 293$ K (isothermal process) and with varying temperature at $P = 1$ bar (isobaric process). Cumene is a simple molecular system. At ambient pressure, it is a "fragile" glass-forming material on an Angel plot of the temperature-dependent viscosity $\eta(T)$ [9]. We have measured the $T = 293$ K pressure dependence of the viscosity $\eta(P)$ up to 14 kbar. Extrapolation to $\eta(P) \simeq 10^{13}$ P of this data through a Tait fit for the pressure-dependent density [1] and a free-volume fit [10] for the density-dependent viscosity yields $P_g \simeq 25$ kbar ($\rho_g \simeq 1.224$ g/cm$^3$). It is also a fragile glass former on an extended Angel plot [11] of the pressure-dependent viscosity.

Depolarized light-scattering measurements were performed in a near-back-scattering ($\theta = 173°$) geometry. The experimental procedure, the Sandercock tandem Fabry-Pérot interferometer, and the Raman apparatus have been described previously [8]. The cumene sample (99%) was obtained from Alfa products. In the variable pressure measurement (VPM), a Merrill-Bassett-type DAC was used. Standard ruby fluorescence techniques were used to measure the pressure in the sample, which was used as supplied by the manufacturer. A complete set of spectra with different free spectral ranges was collected at each pressure before the sample pressure was changed. Because of pressure-induced birefringence in the diamond, leakage of the longitudinal acoustic (LA)

 0031-9007/95/74(12)/2280(4)$06.00 

line from the sample and the diamond Brillouin lines gets stronger at higher pressure. Therefore, our measurements were limited to $P < 8$ kbar. In the variable temperature measurement (VTM), the sample was vacuum distilled and sealed in a glass cell and then placed in an Oxford cryostat. The procedure for splicing together spectra of different spectral ranges has been described in Ref. [8].

In Fig. 1, we show susceptibility spectra from both the VTM (a) and VPM (b). They were obtained by dividing the intensity spectra by the Bose factor. In the VTM, the sample turns slightly milky at low temperatures; therefore, the relative intensity at different temperatures cannot be calibrated. Also, in the VPM, due to the shortening of the scattering column (which is limited by the thickness of the sample between the two diamonds) with increasing pressure, the relative intensity for different pressures cannot be calibrated either. The relative intensities shown in Fig. 1 have been arbitrarily shifted (on a logarithmic scale) for clarity. In Fig. 1(a), the frequency range which contains the small leakage of the LA line due to the imperfect polarizer and the milkiness of the sample at low temperatures has been removed. The small peaks (at ~180 GHz) visible in the spectra of Fig. 1(b) are due to the transverse acoustic modes of the diamond and the birefringence-induced leakage mentioned above. In spite of some small differences, the overall spectral shape and evolution of the spectra shown in Figs. 1(a) and 1(b) are very similar. At low densities (high temperature or low pressure), the low-frequency $\alpha$ relaxation merges with the high-frequency microscopic band. With increasing density (decreasing temperature or increasing pressure), the $\alpha$ relaxation shifts toward lower frequency, and a susceptibility minimum develops between the $\alpha$ peak and the microscopic band.

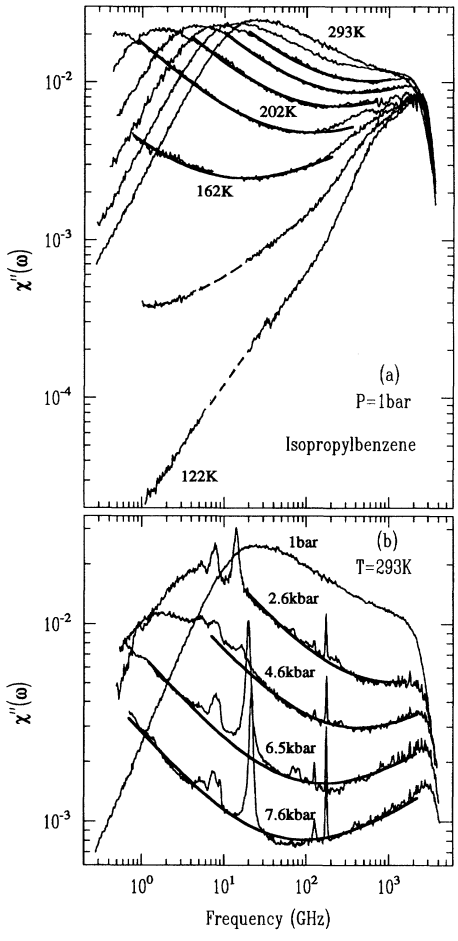


FIG. 1. (a) Susceptibility spectra from the VTM at $P = 1$ bar. The temperatures are: (top to bottom) 293, 263, 242 to 122 K with 20 K per step. (b) Susceptibility spectra from the VPM at $T = 293$ K. The thick solid lines in (a) and (b) are the MCT interpolation fits Eq. (1) with $\lambda$(VTM) = 0.80 and $\lambda$(VPM) = 0.79, respectively. Relative intensities in both data sets are not calibrated.

Within the MCT, the region around the susceptibility minimum corresponds to the fast $\beta$ relaxation which should be approximately described by the interpolation formula

$$\chi''(\omega) \propto b(\omega/\omega_{\min})^a + a(\omega_{\min}/\omega)^b, \quad (1)$$

in which the critical exponents $a$ and $b$ are constrained by the MCT equation

$$\lambda = \Gamma^2(1-a)/\Gamma(1-2a) = \Gamma^2(1+b)/\Gamma(1+2b), \quad (2)$$

where $\lambda$ is a material-dependent constant called the exponent parameter. In Figs. 1(a) and 1(b), we also show the global fits to Eq. (1) with the MCT constraint, Eq. (2), to the VTM and VPM susceptibility spectra, respectively. Note that while the MCT does not require the $\lambda$ values to be the same for the isobaric and isothermal processes [12], the fits yield the same $\lambda$ value [$\lambda$(VTM) = 0.80 ± 0.06 ($a = 0.28$, $b = 0.48$), $\lambda$(VPM) = 0.79 ± 0.06 ($a = 0.29$, $b = 0.49$)] for both data sets. These fits cannot be considered as a proof of the MCT constraint, Eq. (2), because the VTM data lack an extended $\omega^a$ region above the susceptibility minima, and the VPM data are somewhat obstructed by the leakage modes. Nevertheless, the MCT fits shown in Fig. 1 reasonably describe the experimental data around the susceptibility minima.

MCT predicts that near the crossover transition points $T_c$ or $\rho_c$, the frequency of the susceptibility minimum $\omega_{\min}$, the frequency of the susceptibility $\alpha$ peak $\omega_{\max}$, and the viscosity $\eta$ should be described by

$$\omega_{\min} \propto |\sigma|^{1/2a} \quad \text{and} \quad \omega_{\max} \propto (\eta/T)^{-1} \propto |\sigma|^{\gamma} \quad (\sigma < 0), \quad (3)$$

where $\gamma = 1/2a + 1/2b$ and $\sigma$ is the separation parameter. For a VTM, $\sigma \propto (T_c - T)$, and for a VPM, we take $\sigma \propto (\rho_c - \rho)$, where $T_c$ and $\rho_c$ are the crossover temperature and density for the VTM and VPM, respectively. In Figs. 2(a) and 2(b), we plot $\omega_{\min}^{2a}$ and $\omega_{\max}^{1/\gamma}$, and in the inset $[\eta(T)/T]^{-1/\gamma}$ vs $T$ for the VTM and $[\eta(P)/T]^{-1/\gamma}$

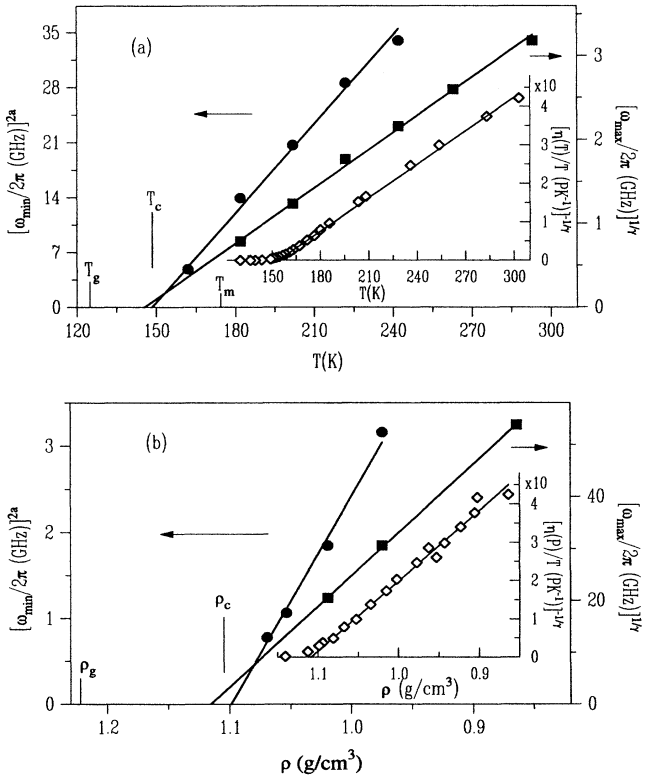


FIG. 2. (a) Temperature dependence of $\omega_{\min}^{2a}$ (circles), $\omega_{\max}^{1/\gamma}$ (squares), and $[\eta(T)/T]^{-1/\gamma}$ (inset) from the VTM. $T_c \simeq 150$ K. (b) Density dependence of $\omega_{\min}^{2a}$ (circles), $\omega_{\max}^{1/\gamma}$ (squares), and $[\eta(P)/T]^{-1/\gamma}$ ($T = 293$ K) (inset) from the VPM. $\rho_c \simeq 1.11$ g/cm$^3$ which corresponds to $P_c \simeq 11$ kbar. Solid lines in (a) and (b) are linear extrapolations.

vs $\rho$ for the VPM, respectively. All three data sets in Fig. 2(a) show linear $T$ dependence, and they extrapolate to a common $T_c \simeq 150$ K. In Fig. 2(b), although there are only a few data points for $\omega_{\max}$ and $\omega_{\min}$ from the VPM, they are essentially linear in $\rho$, and linear extrapolations of the three data sets provide $\rho_c \simeq 1.11$ g/cm$^3$ which corresponds to $P_c \simeq 11$ kbar.

Bengtzelius calculated $T_c(\rho)$ for different densities for a Lennard-Jones (LJ) system [13]. His ($T_c$, $\rho_c$) values lie close to a straight line in the ($T$, $\rho$) plane (see Fig. 1 of Ref. [13]). To compare our results with his, we rescaled his axes so that his $P = 0$ result agrees with our VTM result ($T_c = 150$ K, $\rho_c = 0.982$ g/cm$^3$). We then find that the straight line joining our VTM and VPM ($T_c = 293$ K, $\rho_c = 1.11$ g/cm$^3$) points has a slope of $6.22 \times 10^{-4}$ g/(cm$^3$ K). Compared to $8.95 \times 10^{-4}$ g/(cm$^3$ K) for his result, the agreement is reasonable.

In Fig. 3(a), we show a direct comparison of VTM and VPM susceptibility spectra at the same density, $\rho = 0.972$ g/cm$^3$. Obviously, their spectral shapes are completely different. The $\alpha$ peak and the susceptibility minimum of the VTM spectrum are at much lower

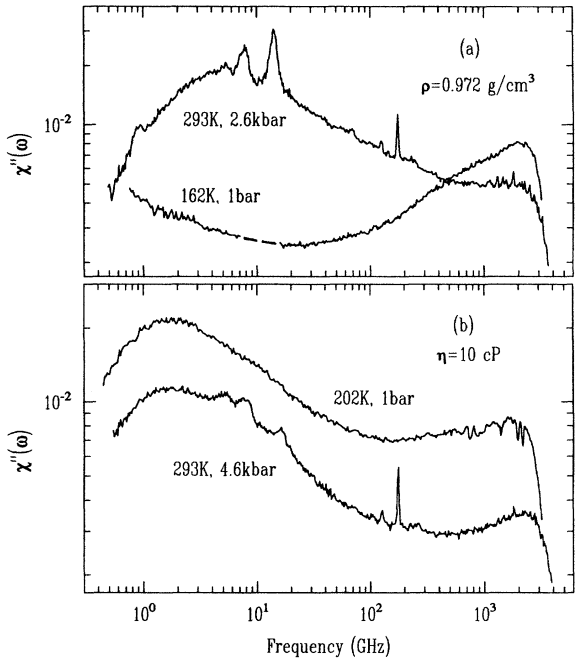


FIG. 3. (a) Comparison of the VTM (162 K, 1 bar) and VPM (293 K, 2.6 kbar) susceptibility spectra at the same density $\rho = 0.972$ g/cm$^3$. (b) Comparison of the VTM (202 K, 1 bar) and VPM (293 K, 4.6 kbar) susceptibility spectra at the same viscosity $\eta \simeq 10$ cP.

frequencies than that of the VPM spectrum. Therefore, it is clear that density is not the only relevant parameter that controls the liquid-glass transition $\beta$ relaxation dynamics. Besides the thermal expansion effect, the temperature has its own direct effect on the relaxation dynamics. Comparison of the temperature and pressure effects on viscosity presents a similar picture [11]. In Fig. 4, $\eta(T)$ [9] and $\eta(P)$ are plotted against $\rho$. One can see that $\eta(T)$ increases with $\rho$ much faster than $\eta(P)$, which provides a reasonable interpretation of the difference shown in Fig. 3(a). A comparison of the VTM and VPM spectra at the same viscosity is shown in Fig. 3(b), for $\eta \simeq 10$ cP. Indeed, in spite of some differences at high frequencies, the spectra are similar in the low-frequency $\alpha$ relaxation region, which suggests that the dynamics of the $\alpha$ relaxation processes in both the isobaric and isothermal experiments are controlled by the combinations of $T$ and $P$ in the same way as the viscosity.

Finally, comparing the spectra shown in Figs. 1(a) and 1(b), one notices that in the VTM, the high-frequency band shows a doublet structure at low temperatures, whereas the VPM spectra show only a single peak. The disappearance of the low-lying peak in the VPM spectra provides a larger frequency range for matching with the MCT $\omega^a$ asymptotic limit. Measurement with a wider frequency range and higher pressure should provide a more accurate test of the MCT predictions. Also, whether

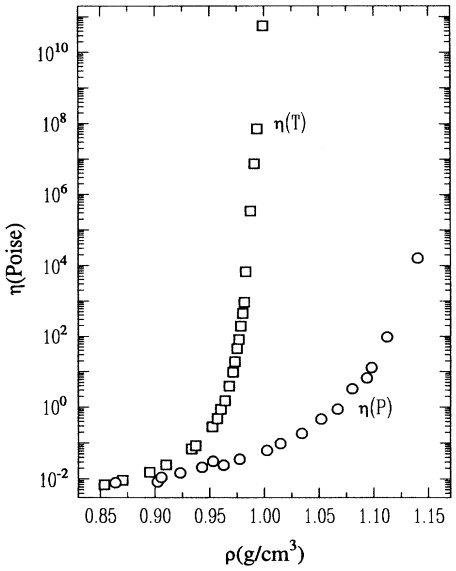


FIG. 4. Density dependence of $\eta(T)$ [9] (squares) and $\eta(P)$ (circles).

the pressure effect suppresses the low-lying peak of the doublet or shifts it to higher frequency is an interesting subject for further investigation.

In summary, a depolarized-light-scattering study of temperature-induced and pressure-induced liquid-glass transitions of isopropylbenzene has revealed that both the supercooled and superpressed liquids show two-step relaxation processes. MCT $\beta$ relaxation theory can reasonably describe the susceptibility spectra in the region of their minima along both paths to the glassy state. Comparison of the VTM and VPM results indicates that density is not the only relevant parameter for the liquid-glass transition dynamics. The effect of temperature on the liquid-glass transition is more than just changing the density through thermal expansion. The $\alpha$ relaxations in the supercooled and superpressed liquids have the same relation to $T$ and $P$ as the corresponding viscosity. Pressure has an additional effect on the high-frequency (boson) peak structure. Further investigation is required to quantify this effect.

We thank W. Götze and M. Fuchs for helpful discussions, and the late R. L. Cook who contributed to the high-pressure viscosity work. Research at City College was supported by the National Science Foundation under Grant No. DMR-9014344.

*Present address: Molten Metal Technology, Inc., Fall River, MA 02720.

[1] P. W. Bridgman, in *Collected Experimental Papers* (Harvard University Press, Cambridge, 1964), Vol. VI.

[2] J. D. Barnett and C. D. Bosco, J. Appl. Phys. **40**, 3144 (1969); G. J. Piermarini, R. A. Forman, and S. Block, Rev. Sci. Instrum. **49**, 1061 (1978); H. E. King, Jr., E. Herbolzheimer, and R. L. Cook, J. Appl. Phys. **71**, 2071 (1992); R. L. Cook, C. A. Herbst, and H. E. King, Jr., J. Phys. Chem. **97**, 2355 (1993).

[3] O. Mishima and E. Whalley, J. Chem. Phys. **84**, 2795 (1986).

[4] W. M. Slie and W. M. Madigosky, J. Chem. Phys. **48**, 2810 (1968); S. Hawley, J. Allegra, and G. Holton, J. Acoust. Soc. Am. **47**, 137 (1970).

[5] W. F. Oliver, C. A. Herbst, S. M. Lindsay, and G. H. Wolf, Phys. Rev. Lett. **67**, 2795 (1991).

[6] W. Götze and L. Sjögren, Rep. Prog. Phys. **55**, 241 (1992).

[7] W. Knaak, F. Mezei, and B. Farago, Europhys. Lett. **7**, 529 (1988); W. Doser, S. Cusack, and W. Petry, Phys. Rev. Lett. **65**, 1080 (1990); J. Wuttke, M. Kiebel, E. Bartsh, F. Fujara, W. Petry, and H. Sillescu, Z. Phys. B **91**, 357 (1993).

[8] G. Li, W. M. Du, X. K. Chen, and H. Z. Cummins, Phys. Rev. A **45**, 3867 (1992); G. Li, W. M. Du, A. Sakai, and H. Z. Cummins, *ibid.* **46**, 3343 (1992); W. Steffen, A. Patkowski, H. Glaser, G. Meier, and E. W. Fischer, Phys. Rev. E **49**, 2992 (1994); W. M. Du, G. Li, H. Z. Cummins, M. Fuchs, J. Toulouse, and L. A. Knauss, Phys. Rev. E **49**, 2192 (1994).

[9] A. J. Barlow, J. Lamb, and A. J. Matheson, Proc. R. Soc. London A **292**, 322 (1966); C. Campbell Ling and J. E. Willard, J. Phys. Chem. **72**, 1918 (1968).

[10] C. A. Herbst, R. L. Cook, and H. E. King, Jr., J. Non-Cryst. Solids **172-174**, 265 (1994).

[11] R. L. Cook, H. E. King, Jr., C. A. Herbst, and D. R. Herschbach, J. Chem. Phys. **100**, 5178 (1994).

[12] W. Götze (private communication).

[13] U. Bengtzelius, Phys. Rev. A **33**, 3433 (1986).